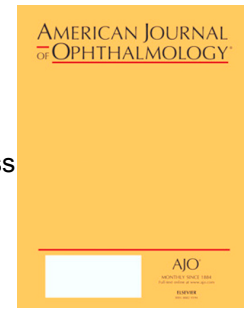

Progression of Retinopathy Secondary to Maternally Inherited Diabetes and Deafness – Evaluation of Predicting Parameters

Philipp L. Müller, Tim Treis, Maximilian Pfau, Simona Degli Esposti, Abdulrahman Alsaedi, Peter Maloca, Konstantinos Balaskas, Andrew Webster, Catherine Egan, Adnan Tufail

PII: S0002-9394(20)30019-2

DOI: https://doi.org/10.1016/j.ajo.2020.01.013

Reference: AJOPHT 11199

To appear in: *American Journal of Ophthalmology*

Received Date: 28 October 2019

Revised Date: 20 December 2019

Accepted Date: 10 January 2020

Please cite this article as: Müller PL, Treis T, Pfau M, Esposti SD, Alsaedi A, Maloca P, Balaskas K, Webster A, Egan C, Tufail A, Progression of Retinopathy Secondary to Maternally Inherited Diabetes and Deafness – Evaluation of Predicting Parameters, *American Journal of Ophthalmology* (2020), doi: https://doi.org/10.1016/j.ajo.2020.01.013.

ABSTRACT:

Purpose: To investigate the prognostic value of demographic, functional, and imaging parameters on retinal pigment epithelium (RPE) atrophy progression secondary to Maternally Inherited Diabetes and Deafness (MIDD) and to evaluate the application of these factors in clinical trial design.

Design: Retrospective observational case series.

Methods: Thirty-five eyes of 20 patients (age range, 24.9-75.9 years) with genetically proven MIDD and demarcated RPE atrophy on serial fundus autofluorescence (AF) images were included. Lesion size and shape-descriptive parameters were longitudinally determined by two independent readers. A linear mixed effect model was used to predict the lesion enlargement rate based on baseline variables. Sample size calculations were performed to model the power in a simulated interventional study.

Results: The mean follow-up time was 4.27 years. The mean progression rate of RPE atrophy was 2.33 mm^2/year revealing a dependence on baseline lesion size (+0.04 [0.02-0.07] mm^2/year/mm^2, $p<0.001$), which was absent after square root transformation. The fovea was preserved in the majority of patients during the observation time. In the case of foveal involvement, the loss of visual acuity lagged behind central RPE atrophy in AF images. Sex, age, and number of atrophic foci predicted future progression rates with a cross-validated mean absolute error of 0.13 mm/year and to reduce the required sample size for simulated interventional trials.

Conclusions: Progressive RPE atrophy could be traced in all eyes using AF imaging. Shape-descriptive factors and patients' baseline characteristics had significant prognostic value, guiding appropriate subject selection and sample size in future interventional trial design.

Progression of Retinopathy Secondary to Maternally Inherited Diabetes and Deafness – Evaluation of Predicting Parameters

Philipp L. Müller,[1,2,3] Tim Treis,[4] Maximilian Pfau,[2,5] Simona Degli Esposti,[1] Abdulrahman Alsaedi,[1,8] Peter Maloca,[1,6,7] Konstantinos Balaskas,[1] Andrew Webster,[1,9] Catherine Egan,[1,9,] Adnan Tufail,[1,9]

[1] *Moorfields Eye Hospital NHS Foundation Trust, London, UK*
[2] *Department of Ophthalmology, University of Bonn, Bonn, Germany*
[3] *Center for Rare Diseases, University of Bonn, Bonn, Germany*
[4] *BioQuant, University of Heidelberg, Heidelberg, Germany*
[5] *Department of Biomedical Data Science, Stanford University, Stanford, USA*
[6] *Institute of Molecular and Clinical Ophthalmology (IOB), Basel, Switzerland*
[7] *OCTlab, Department of Ophthalmology, University Hospital Basel, Switzerland*
[8] *College of Medicine, Imam Mohammad Ibn Saud Islamic University, Riyadh, Saudi Arabia*
[9] *Institute of Ophthalmology, University College London, London, UK*

Financial Support:
This work was supported by the German Research Foundation (grant # MU4279/2-1 to PLM), the United Kingdom's National Institute for Health Research of Health's Biomedical Research Centre for Ophthalmology at Moorfields Eye Hospital and UCL Institute of Ophthalmology. The views expressed are those of the authors, not necessarily those of the Department of Health. The funder had no role in study design, data collection, analysis, or interpretation, or the writing of the report.

Conflict of Interest:
None of the authors has a proprietary interest in this work.

Short Title:
Progression of Retinopathy in MIDD

Keywords:
Retina; MIDD; Fundus Autofluorescence; Imaging; Retinal Pigment Epithelium; Atrophy; Mitochondria

Supplemental Material available at AJO.com

***Corresponding author:**
Adnan Tufail
Moorfields Eye Hospital NHS Foundation Trust,
162 City Rd
London EC1V 2PD
United Kingdom
Telephone: +44 20 7566 2576
E-mail: adnan.tufail@nhs.net

INTRODUCTION

Maternally inherited diabetes and deafness (MIDD, Online Mendelian Inheritance in Man # 520000) was first described in 1992[1] and is primarily caused by mutation in the M*itochondrially Encoded TRNA Leucine 1 (MTTL1)* – gene at position 3243.[2,3] It presents with different ocular and non-ocular phenotypes associated with the individual percentage of affected mitochondria (heteroplasmy).[4–6] The majority (50-85%) of patients reveal a pattern-like dystrophy and/or retinal pigment epithelium (RPE) atrophy at the posterior pole similar to geographic atrophy associated with age-related macular degeneration (AMD), where mitochondrial dysfunction has also been implicated in the pathogenesis.[6]

Although the last decade has witnessed an increase in our understanding of the genetic and biochemical mechanisms underlying many mitochondrial diseases, this has not resulted in effective therapeutic approaches. However, new therapeutic strategies have recently been emerging, some of which have shown potential efficacy at a pre-clinical level and suggestions of promise in early clinical trials.[7] As these pre-clinical therapies enter clinical testing, meaningful, validated clinical endpoints need to be developed. Ideal surrogate markers should be easily captured, reflect the current disease severity and be predictive for long-term progression based on short-term changes. The complexity of the non-ocular disease manifestations such as diabetes, cardiomyopathy, and renal impairment makes it difficult to define reliable surrogate markers.

MIDD can be associated with a maculopathy in 50-85% of patients, [6], taking the form of a bilateral macular pattern dystrophy and/or RPE atrophy.[8] Therefore, MIDD retinal findings may be misdiagnosed with either age-related macular degeneration (AMD) or other retinal dystrophies. MIDD associated RPE atrophy has phenotypic parallels with geographic atrophy in AMD. RPE atrophy may be a suitable endpoint in MIDD patients in the same way that a change of atrophy size is an accepted endpoint by regulators for trials of atrophic AMD.[9,10] However, little is known about either the progression of atrophy or the visual prognosis of MIDD patients

Apart from phenotypic variability, MIDD is rare and would meet orphan diseases designation. To correctly determine treatment effects in future investigational trials, the selection of appropriate participants is crucial. Baseline characteristics and shape descriptive parameters of RPE atrophy have been proposed for the identification of AMD with rapid disease progression using fundus autofluorescence (AF) imaging.[11]

As a more detailed complete reanalysis with longer follow up of the initial dataset,[12] we longitudinally analyzed the size and shape-descriptive factors of RPE atrophy secondary to MIDD using AF imaging. We aimed to evaluate the relevance of demographic, functional, and these lesion geometry factors as prognostic biomarkers to determine RPE atrophy progression in order to perform adapted sample size calculations to enable an effective and economic design of future therapeutic trials.

METHODS

This retrospective observational case series was performed at the Moorfields Eye Hospital, London, United Kingdom. The study was in adherence with the declaration of Helsinki. Approval by the local research governance committee from the Research and Development Department and patients' informed consent was obtained for the study.

Patient selection

Possible participants were identified by text search of electronic medical records from dedicated Medical Retina clinics of the study team at the Moorfields Eye Hospital, London, United Kingdom between 2004 and 2019. The search terms were 'maternally inherited diabetes and deafness', 'MIDD', and 'm.3243A>G'.

The inclusion criteria were defined as (1) presence of the m.3243A>G variant in the *MTTL1*-gene, (2) a compatible phenotype consistent with the clinical diagnoses of MIDD, (3) presence of RPE atrophy defined as demarcated hypoautofluorescent area at 488nm excitation light, and (4) serial AF images with an interval of at least 6 months. In accordance with common use, [13,14] the size of RPE atrophy had to be at least 0.05 mm² (each single atrophic area in cases of multifocality), and the entire lesion must be completely visualized on the AF image at each visit in order to be advanced for analysis. Other retinal pathology and/or AF images inadequate to measure the RPE atrophy (e.g. misalignment and/or insufficient image quality) led to exclusion. If both eyes met the inclusion criteria, both were included.

Imaging

All participants underwent an ophthalmic examination, including best corrected visual acuity (BCVA) testing, slit lamp examination and fundoscopy in routine clinical settings. Prior to multimodal imaging, pupils were dilated. The imaging protocol included spectral-domain optical coherence tomography (OCT, Spectralis HRA+OCT, Heidelberg Engineering, Heidelberg, Germany), and short-wavelength AF imaging (488 nm excitation and 500-700 nm emission) using a different generations of a confocal scanning laser ophthalmoscopy (cSLO; HRA classic, HRA 2, or Spectralis HRA+OCT, Heidelberg Engineering, Heidelberg, Germany) due to availability at the study center at the time of visit. The image resolution was 512 x 512 pixels for the HRA classic, while HRA 2 and Spectralis HRA+OCT recorded images with 768 x 768 pixels (high speed mode) or 1536 x 1536 pixels (high resolution mode). Using the manufacturer's software, up to 100 images (centered to the fovea) were automatically aligned and averaged in order to optimize the signal-to-noise ratio.

Image Processing

Measurements of RPE atrophy lesions were performed by two independent experienced readers (P.L.M. and A.A.), masked to the results of each other, using the semi-automated RegionFinder software (Heidelberg Engineering, Heidelberg, Germany,

version 2.6.3) which has been previously established for retinal degenerations.[13,15] The mean of both reader measures were finally advanced for further analysis.

As previously described,[11] the graded annotated images were exported and transferred to ImageJ (Bethesda, Maryland, USA) to measure the shape-descriptive factors using a custom-built plug-in (Figure 1). In brief, *'Focality'* described the number of atrophic foci with an area ≥ 0.05 mm² in each eye, '*Area'* showed the cumulative size of RPE atrophy, '*Square Root Area'* was calculated as the square root of the '*Area'*, the cumulative circumference of all foci was described by the '*Perimeter'*, '*Circularity'* (i.e. the roundness of the lesion) was calculated by (4×π×Area)/Perimeter², and the maximum and minimum perpendicular distance between parallel tangents touching opposite sides of the lesion was represented by '$Feret_{max}$' and '$Feret_{min}$', respectively. Scaling-factors for the pixel-to-µm conversion were obtained from the HEYEX software (Heidelberg Engineering, Germany).

Statistical analysis

Statistical analyses were performed using the software environment R (version 3.2.3, The R Foundation for Statistical Computing, Vienna, Austria).[16] In order to probe whether square-root transformation reduces the association between lesion area and future progression rate two mixed-effects models were analyzed considering eyes nested in patients as random effects. In the first model, RPE atrophy progression rate (in mm²/year) served as dependent variable and lesion area (in mm²) as independent variable. In the second model, square-root transformed RPE atrophy progression rate (in mm/year) served as dependent variable and lesion area (in mm²) again as independent variable. P-values were based on the Wald tests.

Multiple potential predictors for future (square-root transformed) RPE atrophy progression rates were evaluated using linear mixed-effects models in analogy to Pfau and coworkers.[11] Significant predictors were selected though backward elimination of non-significant effects using P-values for the fixed effects calculated from F tests based on Sattethwaite's approximation. The predictive accuracy of the final model was probed using patient-wise leave-one-out cross-validation (i.e. repeated fitting of the model to n-1 patients and evaluation of the model on the one remaining patient). The cross-validated coefficient-of-determination (R^2) served as measure of model accuracy.

The course of visual acuity over time was analyzed as proposed for retinal dystrophies using Kaplan-Meier curves with Turnbull's estimator.[17,18].

A simulation study for power calculation was performed for possible future interventional trials aiming at slowing RPE atrophy progression. The simulations were done using Mediana, an implementation of the Clinical Scenario Evaluation framework in the R language.[19,20] Clinical trial simulation with 5000 runs each, a significance level of 0.05, a dropout rate of 15 %, and a trial durations of 1-4 years were performed. The statistical

powers for the sample sizes were then extracted as well as the threshold for a power of 80 % was determined.

For evaluation of inter-rater reliability, intraclass correlation coefficients (ICC, two-way random, absolute agreement), 95% coefficients of repeatability (CoR) and coefficients of variation (CV) were determined for lesion size and shape-descriptive factors. Bland-Altman plots were generated for visualization of limits of agreement, and Spearman's rank correlation coefficients (ρ) were calculated between the absolute differences and the mean values to determine whether measurement variability increases with higher mean.

RESULTS

Cohort characteristics

Thirty-five eyes (17 right eyes) of 20 genetically confirmed MIDD patients (13 females, 7 males) were evaluated in the study (Table 1). With a mean age (±SD, years) of 53.5 ± 12.0 (range, 24.9-75.9) and a mean age of onset (i.e. first reported appearance of visual symptoms or retinal alterations) of 48.4 ± 9.1 (range, 21.0-62.0), the mean retinal disease duration was 5.14 ± 4.65 (range, 0.2-15.9) at baseline (i.e. first recorded visit with AF imaging). The age of onset seems to describe a Gaussian distribution with one outliner that reported subjective symptoms significantly earlier (21.0 years, Supplemental Figure 1, Supplemental Material at AJO.com) than the other patients (≥37.2 years).

Baseline Characteristics

While all included patients had been diagnosed with diabetes mellitus years before retinal symptoms, only four eyes (11.4ˆ%) of two patients had diabetic retinopathy at baseline (all graded as mild non-proliferative diabetic retinopathy). Either cataract or pseudophakia was reported in all patients over the age of 50 years which had not been specified in more detail in the records. Two patients were described with cardiovascular complications. Glaucoma was mentioned in two eyes (5.7ˆ%) and Fuch's endothelial dystrophy was detected in one eye (2.9ˆ%).

Twenty (57.1%) of all included eyes revealed a visual acuity of ≤0.1 logMAR (i.e. no impairment). Consistently, a specific distribution of AF alterations including granular pattern as well as RPE atrophy in a circle of 10° to 20° around the foveal center was found in these cases, leaving the fovea evidently uninvolved (Figure 1). Only eight eyes (22.9 %) presented with foveal involving RPE atrophy due to more widespread and confluent lesions. Of note, only one of these eight eyes (12.5 %) revealed a best corrected visual acuity (BCVA) of ≥ 1.0 logMAR (≤ 20/200 Snellen equivalent; severe impairment), whereas 37.5 % and 50 % demonstrated with only moderate (0.6-0.9 LogMAR, 20/80-20/160 Snellen equivalent) or even mild (0.2-0.5 LogMAR, 20/32-20/63 Snellen equivalent) visual impairment, respectively (Figure 2).

As an exception, the eyes of the specific patient with unusual early age of onset revealed a phenotype different from all other patients: (i) A primary foveal involvement of AF alteration, (ii) early severe visual impairment even before presentation of RPE atrophy, and (iii) an unaffected the area of 10° to 20° eccentricity (Supplemental Figure 1, Supplemental Material at AJO.com).

The included eyes showed a wide variability in presentation of the RPE atrophy with ranged from 0.06 mm² to 81.84 mm² for *Area*, 0.24 mm to 9.05 mm for *Square Root Area,* 0.92 mm to 54.09 mm for *Perimeter*, 0.10 to 0.86 for *Circularity*, 0.33 mm to 13.65 mm for $Feret_{max}$, 0.23 mm to 9.54 mm for $Feret_{min}$, and 1 to 7 for *Focality*,

respectively (Table 1). In contrast to the inter-patient variability, there was a high intra-patient agreement between right and left eye when both eyes were included (*Area,* marginal R^2 = 0.820, Figure 1).

There was a correlation of *Area* with age (ρ = 0.450, P = 0.007), disease duration (ρ = 0.632, P < 0.001), and BCVA (ρ = 0.508, P = 0.002) giving the character of a progressive disease. Age of onset (ρ = 0.126, P = 0.479) and foveal status (t-test, P = 0.077) did not show this relationship (Supplemental Figure 2, Supplemental Material at AJO.com).

Progression of RPE Atrophy

Overall, 103 visits have been graded providing 68 unique intervals for evaluation. The follow-up time ranged from 0.52 to 11.57 years with a mean (± standard error of the estimate) of 4.27 ± 2.64 years.

Besides *Area*, increasing values for *Square Root Area, Perimeter*, $Feret_{max}$, and $Feret_{min}$ were found. However, factors describing primarily the lesion shape, such as *Circularity* and *Focality,* overall remained rather constant during the observation time (Table 2). Nevertheless, development of new atrophic spots and coalescing lesions could be observed (Figure 1).

A mixed-effects model analysis (with eyes nested in patients as random effects) revealed that the future "native" *Area* progression rate (i.e. mm^2/year) was significantly dependent on the lesion size (= *Area*, effect estimate [95% CI], +0.04 [0.02 – 0.07] mm^2/year per mm^2, P = 0.001). Square-root transformation of the progression rates (=*Square Root Area*) abolished this association between future progression rates and lesion size (P = 0.500), and was therefore used for further analysis (Supplemental Figure 3, Supplemental Material at AJO.com).

Prediction of Progression Rates

For predictive modeling of future progression rates of *Square Root Area*, all visits were evaluated. Hereby, multiple putative predictors were initially considered including demographic characteristics (sex, age, age of onset, disease duration), functional impairment (BCVA) as well as the multiple lesion-shape-descriptive factors (*Area*, *Square Root Area, Perimeter*, *Circularity*, $Feret_{max}$, $Feret_{min}$, *Focality*, and status of the fovea, presence of peripapillary atrophy). Forward selection revealed that three predictors (sex, age, and *Focality*) predicted future progression rates with a cross-validated mean absolute error (MAE [95% CI]) of 0.13 mm/year [0.10, 0.16]. Of all variables that exhibited a significant effect, higher age was the only variable that also exhibited a significant effect in the multivariate analysis. Hereby, higher age was associated with slightly lower progression rates (estimate [95% CI] -0.01 mm/year per year [-0.01, -0.00], P = 0.025, Supplemental Table 1, Supplemental Material at

AJO.com).

Accordingly, higher progression rates of *Square Root Area* were found in younger patients and in eyes with multifocal presentation of RPE atrophy (Figure 1).The fastest progression rate could be found in the patient with the atypical presentation of age of onset and phenotype, despite the monofocality (Supplemental Figure 1, Supplemental Material at AJO.com). However, the respective patient was the youngest subject in our cohort. In patients with both eyes included, the progression rate revealed a good correlation between right and left eye similar to baseline presentation (Pearson correlation coefficient for *Square Root Area* measures, ρ = 0.652, Figure 1 and Supplement Figure 4, Supplemental Material at AJO.com).

Functional Relevance of RPE Atrophy progression

Using a regression model, time-to-event analysis of patients between baseline and the endpoints ≥ 0.2 LogMAR (≤ 20/32 Snellen equivalent, mild impairment), ≥ 0.6 LogMAR (≤ 20/80 Snellen equivalent, moderate impairment), and ≥ 1.0 LogMAR (≤ 20/200 Snellen equivalent, severe impairment) as well as analysis of the time until onset of foveal involvement could be performed. The 50% cumulative fraction (95% confidence interval) of eyes for reaching the functional endpoints was predicted to be 1.98 (0.19, 4.14), 9.92 (3.75, 16.08) and 9.92 (5.69, 14.14) years after baseline visit, respectively. The 50% cumulative fraction of eyes to reach foveal involvement was predicted to be 6.45 (2.70, 10.21) years after baseline, distinctly earlier than the endpoints 'moderate impairment' and 'severe impairment' (Figure 2 and Figure 3 A). Over the observation time, only the minority of eyes with initial preserved fovea (4/27, 14.8 %) lost the foveal non-involvement. In this cohort of four eyes, only three (75 %) and two (50 %) eyes also reached the endpoints 'moderate impairment' and 'severe impairment'. In contrast, 'mild impairment' was present at or before the visit when foveal involvement was first documented (Figure 3 B).

Inter-Rater Reliability

The image grading of all unique visits by two independent readers (PLM and AA) and following automated evaluations of *Area, Square Root Area, Perimeter*, *Circularity*, $Feret_{max}$, $Feret_{min}$, and *Focality* revealed excellent inter-rater reliability (Table 3). The measurements showed excellent values for ICC and low CV as well as CoR (i.e., with 0.95 probability, the absolute differences between two ratings would lie below this value). Also, the Bland-Altman plots did not reveal systematic inter-rater discrepancies (Figure 4). However, the inter-reader variability significantly increased with larger values for measurements of *Area (*ρ = 0.462, P < 0.001*), Perimeter* (ρ = 406, P < 0.001), *Circularity* (ρ = 308, P = 0.001), $Feret_{max}$ (ρ = 0.281, P = 0.004), and $Feret_{min}$ (ρ = 0.419, P < 0.001) according to Spearman's rank correlation coefficient (ρ) for absolute differences and mean values. *Square Root Area* (ρ = -0.027, P = 0.785), and *Focality* (ρ

= 0.165, P = 0.095) did not show this correlation.

Sample Size Calculation

The observed progression kinetics allowed sample size calculations for future therapeutic trials with an expected reduction to 30%, 40%, 50%, 60% and 70% progression rates of *Square Root-Area* depending on the desired power and trial duration. As the progression rates were assumed to be depend on different key characteristics, we differentiated 5 different scenarios based on the above presented results concerning the predictive value of the baseline data and pretests (Supplemental Figure 5 and Supplemental Table 2, Supplemental Material at AJO.com): I) Evaluating without prior patient selection (Figure 5 A und F); II) evaluating only eyes from patients over the age of 55 (Figure 5 B and G), III) evaluating only eyes from patients under the age of 55 (Figure 5 C and H), IV) evaluating only eyes from patients with monofocality (Figure 5 D and I), and V) evaluating only eyes from patients with multifocality at baseline (Figure 5 E and J). Data of patients with two included eyes (30 eyes from 15 patients) were analyzed for the calculations, so that one eye could serve as control while the other one was treated.[18] The necessary sample size significantly reduced with an extension of the trial duration (with most effect from one to two years) and proposed patient selection (II-V) giving a more homogenous progression rate with minimized interindividual deviations. To obtain a statistical power of ≥ 0.8 during a two-year trial assuming a 50% therapeutic effect (30%, 70%) in case I, at least 9 (17, 8) patients with bilateral RPE atrophy would be required. In case II, at least 6 (11, 3), for III) at least 6 (10, 3), for IV) at least 8 (12, 3), and for V) at least 8 (13, 3) patients would be sufficient. To account for systemic treatment effects, a further sample size calculation was performed for a combined effect on both eyes of individual patients on the basis of data of the whole cohort (35 eyes of 20 patients). Results can be found in Supplemental Figure 6 (Supplemental Material at AJO.com)

DISCUSSION

This is the first study to systematically investigate different shape descriptive parameters of RPE atrophy secondary to a monogenetic mitochondrial disorder as prognostic biomarkers for disease progression. The presented findings provided evidence for the prognostic relevance of demographic characteristics, phenotype and shape-descriptive factors at baseline. With adequate patient selection, future interventional trials could be realized in a more effective manner, as a sufficient statistical power may be achieved with a relatively small sample size.

Presentation of Retinopathy in MIDD

The presentation, variability and rate of expansion of RPE atrophy in MIDD was comparable to reported data in AMD, which might suggest similarities in terms of pathogenesis.[11,21] However, the typical location of retinal abnormalities in MIDD at 10° to 20° eccentricity differs from AMD or other macular dystrophies, that usually develop more centrally.[21] The combination of this relatively peripheral disease manifestation with the described progression kinetics of the RPE atrophy (slower centripetal compared to centrifugal progression, similar to AMD)[22] explains the high number of foveal sparing in our MIDD cohort, which in turn is associated with unusual long lasting preserved visual acuity (Figure 1).

Ophthalmologists should be aware of similarities and distinguishing features between MIDD and AMD: From a clinical point of view, MIDD is associated with non-ocular features including diabetes, cardiomyopathy, and renal disease that might be life threatening, that underlines the importance of the distinction between MIDD and other macular atrophy associated disorders such as AMD and PRPH2 dystrophy.[6,23]

Multifactorial diseases, like AMD, are driven by heterogeneous risk factors, making it problematic as an entity for proof-of-concept studies that may target just a specific pathogenic pathway. Given the unclear role of mitochondrial dysfunction in AMD and the aging retina/RPE, a potential approach to evaluating therapeutics focusing on mitochondrial dysfunction might be to evaluate these strategies first in a model disease for primary mitochondriopathy like MIDD and, if proven, then moving to a proof of concept atrophic AMD trial. There are a number of specific and non-specific therapeutics aimed at treating various mitochondrial disorders and the sample size estimates demonstrated that an orphan disease study could be undertaken with relatively small numbers assuming a reasonably efficacious treatment.

Pathophysiologic considerations

The phenotype and the severity of disease manifestation in MIDD has been associated with the percentage of mtDNA mutations in the respective tissue.[4] As this percentage increases with aging,[2] a correlation between age and lesion size respectively annual

progression rate was shown. In this context, our data also indicated a distinct relationship between progression rates and baseline area of RPE atrophy, similar to previous findings in other retinal diseases.[11,24] Explanations this quasi-exponential relationship might derive from a cascading process at the lesion boundary that drives the RPE atrophy progression in retinal diseases. Accordingly, histopathologic studies in AMD were able to confirm that the percentage of abnormal RPE cells and intraretinal abnormalities increased toward the atrophic lesion.[25,26] With increasing size, the border of the lesion enlarges, explaining the higher progression rate.[11,15] Even after square-root transformation, the number of atrophic spots (*Focality*) was prognostic, hence not significant in multivariate analyses, for the progression rates as they might represent the severity of altered RPE cells and increase the amount of lesion border. To our knowledge, the location of typical retinal abnormalities in MIDD at 10° to 20° eccentricity is unique to MIDD. This particular 'MIDD area' represents the retinal region with the highest density of rod photoreceptors.[27] Of note, some patients have described problems in dark adaptation and night vision as initial symptoms. Future investigation of dark adaptation and specific rod function might give further insights into this particular pathogenic pathway. A different phenotype of MIDD, primarily affecting the central posterior pole was associated with young age of onset, early visual impairment, and higher progression rate in a single case (Supplemental Figure 1, Supplemental Material at AJO.com). Future multicenter studies with larger cohorts might provide more knowledge into the background and frequency of different disease manifestations.

The choroid and the RPE cell monolayer have been shown to represent a functional complex, where diffusible factors from the RPE sustain the choroidal structure and vice versa. Therefore, choriocapillaris atrophy has been reported to be associated with atrophy of the RPE and photoreceptors in a variety of retinal diseases.[28–32] Future analysis of choroidal OCT layers in MIDD, would therefore be of great interest to model disease progression and refine further clinical trial design. The interval between central involvement of RPE atrophy and associated loss of visual acuity further raises the need for OCT studies to investigate the retinal layers in association with the formation of RPE atrophy (Figure 2). Giving our findings of this AF study, we might hypothesize that RPE atrophy precedes photoreceptor cell death indicating MIDD (and therefore mitochondrial diseases) primarily affects the RPE rather than photoreceptors or other retinal cells. This would have implications for the way these disease entities should be approached by therapeutically, such as RPE cell transplants.

Relevance for assessment of progression and treatment effects

The variability of non-ocular features of MIDD, and the complexity of determining a robust endpoint for features such as diabetes, cardiomyopathy, and renal disease may be difficult, Therefore, an easy to measure, continuous variable may aid the development of clinical trials and potentially act as a primary endpoint. Apart from preterm cataract, typical ocular disease manifestations are pattern dystrophy-like alterations and RPE atrophy.[6,23] Due to the typical distribution of these retinal alterations

at 10° to 20° eccentricity (Figure 1),[6] best corrected visual acuity, a central foveal function, does also not constitute a useful endpoint because it usually stays stable over many years up to advanced stages as described in our cohort (Figure 3). However, the retinal alterations might reflect the current disease severity and are an easy to measure continuous variable. These changes (i.e., pattern dystrophy-like alterations and RPE atrophy) are different from typical findings in diabetic retinopathy, which was absent in the majority of our cohort despite up to decades of diabetes mellitus. The exact mechanism preventing diabetic retinopathy in MIDD are still unclear and open for further investigations. In contrast, all patients over a distinct age presented either cataract or pseudophakia, earlier than you would expect in general population.[33,34] The presence of cataract may interfere with retinal imaging and should be factored into trial design when considering recruitment. Analogous to recent natural history studies and/or interventional trials for retinal diseases, we relied on RPE atrophy in this study as it had been approved as reliable endpoint by regulators for other retinal degenerations.[9,10] For MIDD, we could show that the lesion size and geometry of RPE atrophy are easy to measure as continuous variables with excellent inter-rater agreements similar to other retinal diseases like AMD or Stargardt disease.[11,15]

Our data also indicated a distinct relationship between progression rates and baseline area of RPE atrophy, similar to previous findings in other retinal diseases.[11,24] We could show that this quasi-exponential progression kinetics of the lesion size was eliminated with square root transformation. Square root transformation also minimizes and even reversed the correlation between age and annual progression rate. Accordingly, square root transformation abolishes the need to adjust for lesion size and/or limit the inclusion to a specific range of lesion sizes, which might facilitate the conduct of future clinical trials.

The systematic evaluation of shape-descriptive factors of RPE atrophy is relatively novel with only few reports focusing on AMD and *ABCA4*-related retinopathy.[11,15,35] As RPE atrophy grading is already part of the eligibility assessment of currently ongoing studies for many retinal diseases, the evaluation of lesion geometry could be performed fully-automated. These shape-descriptive (especially *Focality*) and further demographic (age and sex) parameters allowed for a more accurate prediction of progression rates compared to currently used selection criteria. By defining more homogenous study cohorts, we could demonstrate that the sample size and trial duration to allow for significant results of an expected fixed treatment effect could be significantly reduced.

The utilization of Region Finder or equivalent software, will have a lower reliability of size measurement with larger lesions due to the used algorithm, as found in this study and studies for Stargardt disease and AMD related atrophy.[14,15] Overall, the high variability of phenotypic manifestation did not influence the inter-rater agreement, indicating that RPE atrophy may potentially act as a primary endpoint and aid the development of clinical trials for MIDD. Of note, the inclusion of eyes with either very large or very small atrophic lesions might have resulted in markedly improved ICC irrespective of the underlying grading method. To enable a more meaningful comparability with different study cohorts, we used the CR as it is independent of the average lesion size.[36]

Limitations and outlook

The use of short-wavelength AF has raised concerns due to the theoretical phototoxicity and wavelength-dependent light absorption by xanthophylls and optical media opacities.[37,38] However, no human harm has been shown. Nevertheless, reduced image quality and shadowing due to light absorption by xanthophylls and optical media opacities might be an important factor when dealing with MIDD, giving the early presence of cataract in our cohort. Especially in clinical trials, it is crucial to maximize the inter-rater agreement, because effect sizes and therefore sample size determinations are dependent on the underlying measurement variability.[36] It has been shown for different retinal diseases that inter-rater agreement increases (especially for small central lesions) using AF imaging with higher excitation wavelength (i.e., green light AF) because of less absorption and increment of patient comfort during the examination.[15,39–41] This AF modality could be of interest in future MIDD imaging studies.

Conclusion and impact of the study

In view of the high inter-rater agreement, the progression of RPE atrophy secondary to MIDD assessed by AF images might be a possible short-term surrogate marker for disease progression and treatment effects in future clinical trials. Demographic, phenotypic and shape-descriptive factors were shown to be prognostic variables for the progression rate. Including these parameters in patient selection would allow for a more accurate prognosis and allow for a significant reduction of the sample size for future interventional trials which is inevitable giving the rarity of this disease. This study demonstrates that a clinical trial using reduction in RPE atrophy enlargement in MIDD may allow for a clean proof of concept clinical trial endpoint. As MIDD is a clean model disease for mitochondrial dysfunction, patients suffering from more common multifactorial retinal conditions where mitochondrial dysfunction has been implicated, might benefit if proof of concepts for pathogenetic pathways and mitochondrial therapies can be established in this disease model.

ACKNOWLEDGEMENTS / DISCLOSURES

Support: This work was supported by the German Research Foundation (grant # MU4279/2-1 to PLM), the United Kingdom's National Institute for Health Research of Health's Biomedical Research Centre for Ophthalmology at Moorfields Eye Hospital and UCL Institute of Ophthalmology. The views expressed are those of the authors, not necessarily those of the Department of Health. The funder had no role in study design, data collection, analysis, or interpretation, or the writing of the report.

Conflict of Interest: No financial disclosures exist for any author.

Other contributors: We thank Rengin Kurt (Memorial Health Group Sisli Hospital, İstanbul, Turkey) for her support in the initial work that led to this study.

REFERENCES

1. Reardon W, Ross RJ, Sweeney MG, et al. Diabetes mellitus associated with a pathogenic point mutation in mitochondrial DNA. *Lancet (London, England)*. 1992;340(8832):1376-1379.

2. Hart LM 't, Jansen JJ, Lemkes HHPJ, de Knijff P, Maassen JA. Heteroplasmy levels of a mitochondrial gene mutation associated with diabetes mellitus decrease in leucocyte DNA upon aging. *Hum Mutat*. 1996;7(3):193-197.

3. Naing A, Kenchaiah M, Krishnan B, et al. Maternally inherited diabetes and deafness (MIDD): Diagnosis and management. *J Diabetes Complications*. 2014;28(4):542-546.

4. Feigl B, Morris CP. Visual function and risk genotypes in maternally inherited diabetes and deafness. *Can J Ophthalmol*. 2013;48(5):e111-4.

5. van den Ouweland JM, Lemkes HH, Trembath RC, et al. Maternally inherited diabetes and deafness is a distinct subtype of diabetes and associates with a single point mutation in the mitochondrial tRNA(Leu(UUR)) gene. *Diabetes*. 1994;43(6):746-751.

6. Massin P, Virally-Monod M, Vialettes B, et al. Prevalence of macular pattern dystrophy in maternally inherited diabetes and deafness. GEDIAM Group. *Ophthalmology*. 1999;106(9):1821-1827.

7. Viscomi C, Bottani E, Zeviani M. Emerging concepts in the therapy of mitochondrial disease. *Biochim Biophys Acta - Bioenerg*. 2015;1847(6-7):544-557.

8. Massin P, Guillausseau PJ, Vialettes B, et al. Macular pattern dystrophy associated with a mutation of mitochondrial DNA. *Am J Ophthalmol*. 1995;120(2):247-248.

9. Csaky KG, Richman EA, Ferris FL. Report from the NEI/FDA Ophthalmic Clinical Trial Design and Endpoints Symposium. *Invest Ophthalmol Vis Sci*. 2008;49(2):479-489.

10. Holz FG, Strauss EC, Schmitz-Valckenberg S, van Lookeren Campagne M. Geographic atrophy: clinical features and potential therapeutic approaches. *Ophthalmology*. 2014;121(5):1079-1091.

11. Pfau M, Lindner M, Goerdt L, et al. Prognostic Value of Shape-Descriptive Factors for the Progression of Geographic Atrophy Secondary to Age-Related Macular Degeneration. *Retina*. 2019;39(8):1527-1540.

12. Esposti SD, Cilkova M, Kurt RA, et al. Atrophy progression on autofluorescence in patients with Maternally Inherited Diabetes and Deafness (MIDD). *Invest Ophthalmol Vis Sci*. 2016;57:1704-1704.

13. Schmitz-Valckenberg S, Brinkmann CK, Alten F, et al. Semiautomated Image Processing Method for Identification and Quantification of Geographic Atrophy in Age-Related Macular Degeneration. *Investig Opthalmology Vis Sci*. 2011;52(10):7640-7646.

14. Kuehlewein L, Hariri AH, Ho A, et al. Comparison of Manual and Semiautomated Fundus Autofluorescence Analysis of Macular Atrophy in Stargardt Disease Phenotype. *Retina*. 2016;36(6):1216-1221.

15. Müller PL, Pfau M, Mauschitz MM, et al. Comparison of Green Versus Blue Fundus Autofluorescence in ABCA4 -Related Retinopathy. *Transl Vis Sci Technol*. 2018;7(5):13.

16. R CT. R: A language and environment for statistical computing. R Foundation for Statistical Computing. 2015.

17. Giolo SR. *Turnbull's Nonparametric Estimator for Interval-Censored Data'*.; 2004.

18. Lambertus S, Lindner M, Bax NM, et al. Progression of Late-Onset Stargardt Disease. *Investig Opthalmology Vis Sci*. 2016;57(13):5186–5191.

19. Paux G, Dmitrienko A. Mediana: Clinical Trial Simulations. R package version 1.0.8. 2019.

20. Friede T, Nicholas R, Stallard N, et al. Refinement of the Clinical Scenario Evaluation Framework for Assessment of Competing Development Strategies with an Application to Multiple Sclerosis. *Drug Inf J*. 2010;44(6):713-718.

21. Fleckenstein M, Mitchell P, Freund KB, et al. The Progression of Geographic Atrophy Secondary to Age-Related Macular Degeneration. *Ophthalmology*. 2018;125(3):369-390.

22. Lindner M, Böker A, Mauschitz MM, et al. Directional Kinetics of Geographic Atrophy Progression in Age-Related Macular Degeneration with Foveal Sparing. *Ophthalmology*. 2015;122(7):1356-1365.

23. Daruich A, Matet A, Borruat F-X. Macular dystrophy associated with the mitochondrial DNA A3243G mutation: pericentral pigment deposits or atrophy? Report of two cases and review of the literature. *BMC Ophthalmol*. 2014;14:77.

24. Feuer WWJ, Yehoshua Z, Gregori G, et al. Square root transformation of geographic atrophy area measurements to eliminate dependence of growth rates on baseline lesion measurements: a reanalysis of age-related eye disease study report no. 26. *JAMA Ophthalmol*. 2013;131(1):110-111.

25. Zanzottera EC, Ach T, Huisingh C, Messinger JD, Spaide RF, Curcio CA. Visualizing retinal pigment epithelium phenotypes in the transition to geographic atrophy in age-related macular degeneration. *Retina*. 2016;36 Suppl 1:S12-S25.

26. Sarks JP, Sarks SH, Killingsworth MC. Evolution of geographic atrophy of the retinal pigment epithelium. *Eye*. 1988;2(Pt 5):552-577.

27. Goldstein EB. *Wahrnehmungspsychologie*. 2nd ed. (Ritter M, ed.). Heidelberg: Spektrum Akademischer Verlag; 2002.

28. Müller PL, Fimmers R, Gliem M, Holz FG, Charbel Issa P. Choroidal Alterations in ABCA4-Related Retinopathy. *Retina*. 2017;37(2):359-367.

29. Adhi M, Read SP, Ferrara D, Weber M, Duker JS, Waheed NK. Morphology and Vascular Layers of the Choroid in Stargardt Disease Analyzed Using Spectral-Domain Optical Coherence Tomography. *Am J Ophthalmol*. 2015;160(6):1276-1284.e1.

30. Müller PL, Pfau M, Möller PT, et al. Choroidal Flow Signal in Late-Onset Stargardt Disease and Age-Related Macular Degeneration: An OCT-Angiography Study. *Invest Ophthalmol Vis Sci*.

2018;59(4):AMD122-AMD131.

31. Kurihara T, Westenskow PD, Bravo S, Aguilar E, Friedlander M. Targeted deletion of Vegfa in adult mice induces vision loss. *J Clin Invest*. 2012;122(11):4213-4217.

32. Lindner M, Bezatis A, Czauderna J, et al. Choroidal Thickness in Geographic Atrophy Secondary to Age-Related Macular Degeneration. *Invest Ophthalmol Vis Sci*. 2015;56(2):875-882.

33. Kanthan GL, Wang JJ, Rochtchina E, et al. Ten-Year Incidence of Age-Related Cataract and Cataract Surgery in an Older Australian Population. *Ophthalmology*. 2008;115(5):808-814.e1.

34. Klein BEK, Klein R, Lee KE. Incidence of age-related cataract over a 10-year interval: the Beaver Dam Eye Study. *Ophthalmology*. 2002;109(11):2052-2057.

35. Domalpally A, Danis RP, White J, et al. Circularity index as a risk factor for progression of geographic atrophy. *Ophthalmology*. 2013;120(12):2666-2671.

36. Bland JM, Altman D. Statistical methods for assessing agreement between two methods of clinical measurement. *Lancet*. 1986;327(8476):307-310.

37. Boettner EA, Wolter JR. Transmission of the Ocular Media. *Invest Ophthalmol Vis Sci*. 1962;1(6):776-783.

38. Müller PL, Müller S, Gliem M, et al. Perception of Haidinger Brushes in Macular Disease Depends on Macular Pigment Density and Visual Acuity. *Invest Ophthalmol Vis Sci*. 2016;57(3):1448-1456.

39. Pfau M, Goerdt L, Schmitz-Valckenberg S, et al. Green-Light Autofluorescence Versus Combined Blue-Light Autofluorescence and Near-Infrared Reflectance Imaging in Geographic Atrophy Secondary to Age-Related Macular Degeneration. *Investig Opthalmology Vis Sci*. 2017;58(6):121-130.

40. Sparrow JR, Nakanishi K, Parish CA. The lipofuscin fluorophore A2E mediates blue light-induced damage to retinal pigmented epithelial cells. *Invest Ophthalmol Vis Sci*. 2000;41(7):1981-1989.

41. Cideciyan A V, Swider M, Aleman TS, et al. Reduced-illuminance autofluorescence imaging in ABCA4-associated retinal degenerations. *J Opt Soc Am A*. 2007;24(5):1457–1467.

FIGURE CAPTIONS

Figure 1: Presentation and Progression of RPE Atrophy

Fundus autofluorescence images of four exemplary patients are demonstrated that revealed high (A and B, top) and low (C and D, bottom) *Square Root Area* progression rates. Values indicate *Area* (upper value) and *Square Root Area* (lower value). While *Area* progression rates systematically increases over time (B and D, associated with increasing lesion size), *Square Root Area* progression rates stayed more constant. Both eyes of each patient revealed comparable RPE atrophy presentation and progression rates. The fast progressing eyes (A and B) usually were of younger age (here, 49.9 and 50.1 years at baseline) and typically revealed multiple spots of atrophic lesions. Both slow progressing patients were of higher age (75.9 and 63.2 years at baseline) and revealed either unifocal RPE atrophy (C) or a low number of atrophic spots with smooth borders (D). Of note, during disease progression development of new atrophic spots and coalescing lesions could be observed.

Figure 2: Functional impairment and foveal involvement of RPE Atrophy

Fundus autofluorescence images and associated best corrected visual acuity of an exemplary eye that demonstrated prolonged preserved visual function despite loss of foveal integrity.

Figure 3: Course of visual impairment.

The time-to-event curves show the cumulative fraction of eyes reaching the following clinical endpoints: ‘Mild visual impairment’ (≥0.2 LogMAR, ≤ 20/32 Snellen equivalent brown solid line), ‘moderate visual impairment’ (≥0.6 LogMAR, ≤ 20/80 Snellen equivalent, pink dashed line), ‘severe visual impairment’ (≥1.0 LogMAR, ≤ 20/200 Snellen equivalent, blue dotted line), and ‘foveal involving RPE atrophy’(dark grey dot-dashed line). Analysis was done for all eyes in the dataset (A) and eyes with preserved foveal integrity at the beginning of the study (B). Foveal involvement seemed to occur before moderate or severe visual impairment was observed.

Figure 4: Inter-Rater Agreement.

The Bland-Altman plots demonstrate the inter-rater agreement of the measurements of the lesion size (*Area*, A), the cumulative circumference (*Perimeter*, B), the roundness of the lesion (*Circularity*, C) the maximal ($Feret_{max}$, D) and minimal ($Feret_{min}$, E) perpendicular distance between parallel tangents touching opposite sides of the lesion, and the number of atrophic spots (*Focality*, F). Measurement differences of both readers are plotted against their mean. The solid line indicates the mean difference and

the dashed lines indicate the 95% limits of agreement. There were no systematic differences between the readers.

Figure 5: Sample-Size Calculations.

Sample size calculations are shown for an expected treatment effect of 70 %, 60 %, 50 %, 40 %, and 30 % reduction of *Square Root Area* progression in patients with bilateral DDAF lesions for a trial duration of 2 years (A-E). Additionally, the minimal sample size required for a statistical power greater or equal to 80 % for the aforementioned expected treatment effects as a function of treatment duration are shown (F-J). Symbols indicate data points predicted by the clinical trial simulation, the respective lines show a fit of the corresponding data points. The minimal sample sizes were calculated based on the fits to achieve a more fine-grained resolution. Panels A and F show the results of simulations based on all patients with two eyes within the data, assuming treatment for one eye while the other serves as a control. Furthermore, the aforementioned data was split into four subgroups based on baseline parameters: Eyes of patients equal to or older than 55 years (B & G), eyes of patients younger than 55 (C & H), eyes with monofocal RPE atrophy (D & I), and eyes with multifocality (E & J) at the first assessment.

Table 1: Demographic, functional, and lesion geometry parameters at baseline

	Parameter	Baseline Data
Patient-level data	Eyes/Patients [n]	35/20
	Females [n, eyes/patients]	22/13
	Males [n, eyes/patients]	13/7
	Age [years] [a]	53.5 ± 12.0
	Age of retinal onset [years] [a]	48.4 ± 9.1
	Retinal disease duration [years] [a]	5.14 ± 4.65
Eye-level data	Best corrected visual acuity [LogMAR]*	0.19 ± 0.27
	Area [mm²] [b]	9.73 [3.64, 26.65]
	Square-Root Area [mm] [b]	3.12 [1.90, 5.16]
	Perimeter [mm] [b]	24.49 [16.68, 29.28]
	Circularity [AU] [b]	0.26 [0.19, 0.41]
	$Feret_{max}$ [mm] [b]	6.01 [5.37, 7.11]
	$Feret_{min}$ [mm] [b]	4.68 [3.22, 5.96]
	Focality [AU] [b]	2.5 [1, 4]

[a] Values indicate mean ± standard deviation

[b] Values indicate median [first quantile, third quantile]

LogMAR = Logarithm of the Minimum Angle of Resolution

Table 2: Progression rates of lesion geometry parameters

Parameter	Estimate	95% CI	P-value
Area [mm²/year]	2.33	1.64 – 3.03	<0.001
Square-Root Area [mm/year]	0.29	0.23 – 0.35	<0.001
Perimeter [mm/year]	1.53	0.55 – 2.50	0.002
Circularity [AU/year]	0.02	0.00 – 0.04	0.100
$Feret_{max}$ [mm/year]	0.30	0.23 – 0.37	<0.001
$Feret_{min}$ [mm/year]	0.31	0.24 – 0.37	<0.001
Focality [AU/year]	-0.04	-0.28 – 0.20	0.725

CI = Confidential Interval

Table 3: Inter-rater agreement

Grading parameter	CoR	CV [%]	ICC (95% CI)
Area	0.877 mm²	1.24	0.999 (0.999 – 0.999)
Square-root Area	0.088 mm	0.71	0.999 (0.999 – 0.999)
Perimeter	3.821 mm	4.60	0.990 (0.984 – 0.993)
Circularity	0.067 [AU]	8.04	0.978 (0.967 – 0.985)
$Feret_{max}$	0.291 mm	1.45	0.999 (0.998 – 0.999)
$Feret_{min}$	0.277 mm	1.85	0.999 (0.998 – 0.999)
Focality	0.547 [AU]	7.56	0.988 (0.983 – 0.992)

CoR = 95% coefficients of repeatability, CV = coefficients of variation, ICC = Intraclass correlation coefficients

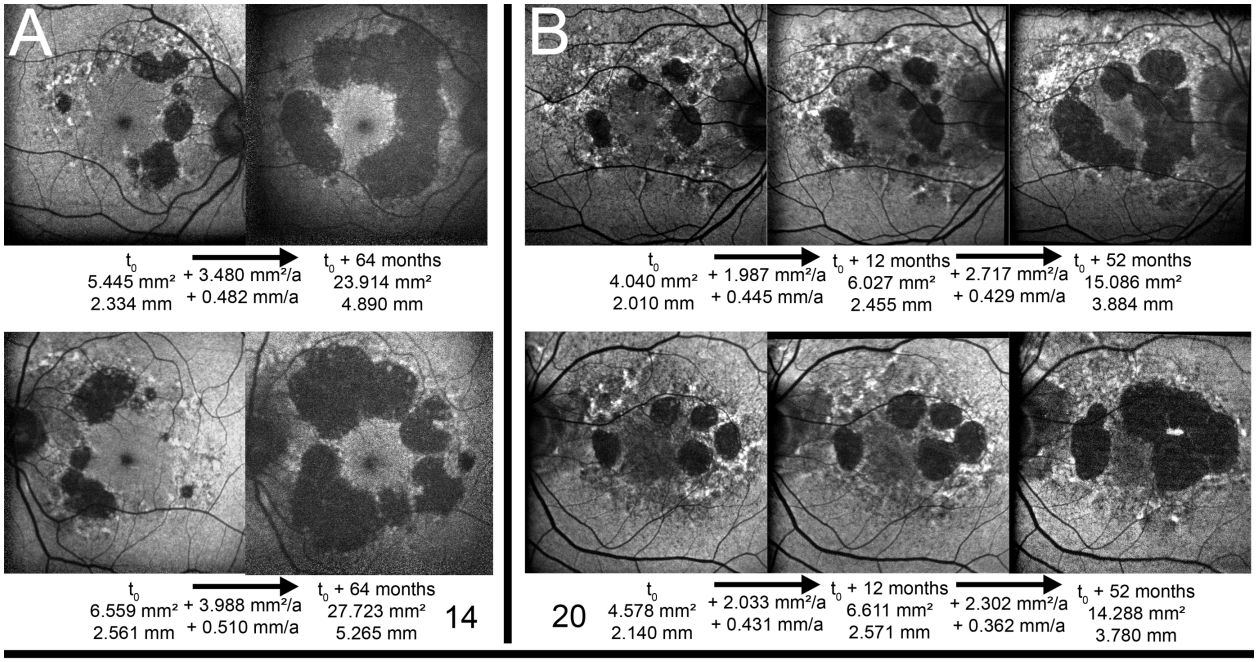
A
t_0
5.445 mm²
2.334 mm
+ 3.480 mm²/a
+ 0.482 mm/a
t_0 + 64 months
23.914 mm²
4.890 mm
t_0
6.559 mm²
2.561 mm
+ 3.988 mm²/a
+ 0.510 mm/a
t_0 + 64 months
27.723 mm²
5.265 mm
14
B
t_0
4.040 mm²
2.010 mm
+ 1.987 mm²/a
+ 0.445 mm/a
t_0 + 12 months
6.027 mm²
2.455 mm
+ 2.717 mm²/a
+ 0.429 mm/a
t_0 + 52 months
15.086 mm²
3.884 mm
20
t_0
4.578 mm²
2.140 mm
+ 2.033 mm²/a
+ 0.431 mm/a
t_0 + 12 months
6.611 mm²
2.571 mm
+ 2.302 mm²/a
+ 0.362 mm/a
t_0 + 52 months
14.288 mm²
3.780 mm

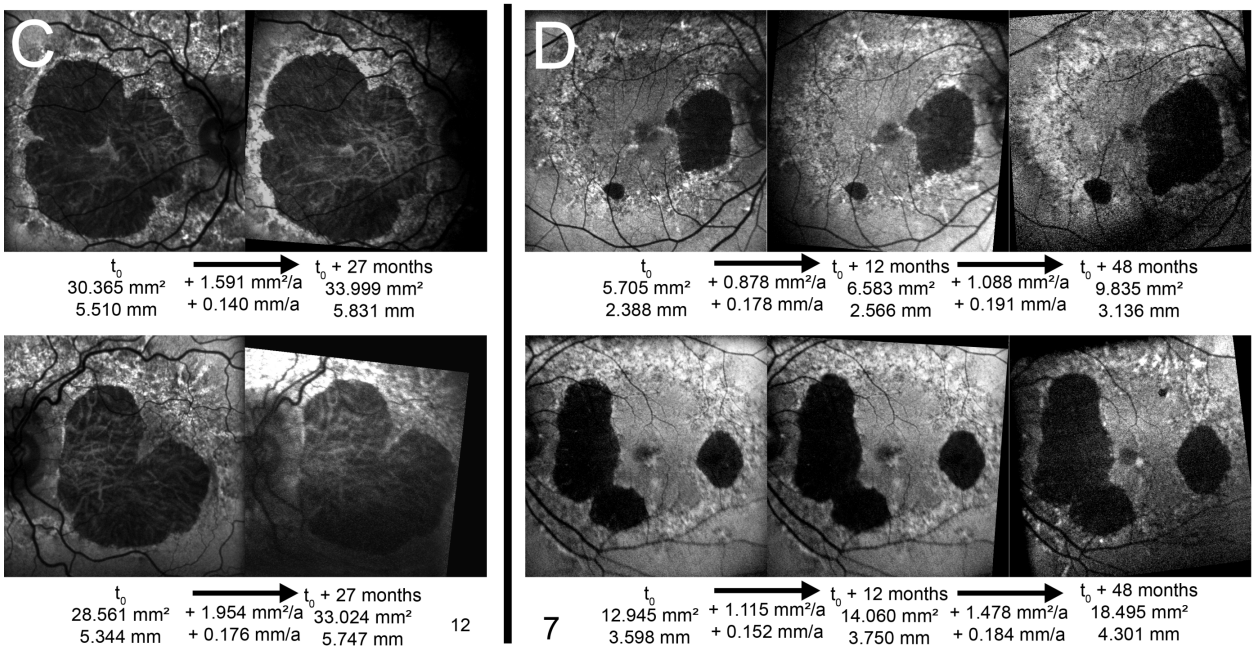
C
t_0
30.365 mm²
5.510 mm
+ 1.591 mm²/a
+ 0.140 mm/a
t_0 + 27 months
33.999 mm²
5.831 mm
t_0
28.561 mm²
5.344 mm
+ 1.954 mm²/a
+ 0.176 mm/a
t_0 + 27 months
33.024 mm²
5.747 mm
12
D
t_0
5.705 mm²
2.388 mm
+ 0.878 mm²/a
+ 0.178 mm/a
t_0 + 12 months
6.583 mm²
2.566 mm
+ 1.088 mm²/a
+ 0.191 mm/a
t_0 + 48 months
9.835 mm²
3.136 mm
7
t_0
12.945 mm²
3.598 mm
+ 1.115 mm²/a
+ 0.152 mm/a
t_0 + 12 months
14.060 mm²
3.750 mm
+ 1.478 mm²/a
+ 0.184 mm/a
t_0 + 48 months
18.495 mm²
4.301 mm

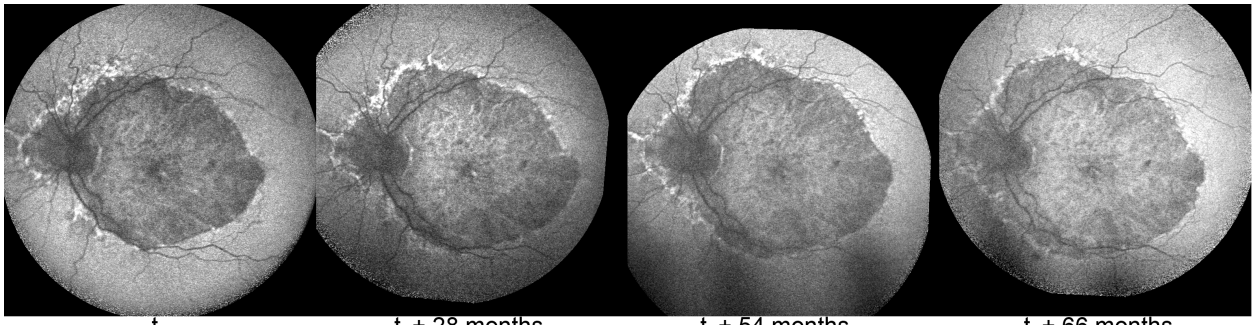

t_0	t_0 + 28 months	t_0 + 54 months	t_0 + 66 months
0.5 LogMAR	0.7 LogMAR	1.0 LogMAR	1.2 LogMAR
20/63 Snellen	20/100 Snellen	20/200 Snellen	20/320 Snellen

A

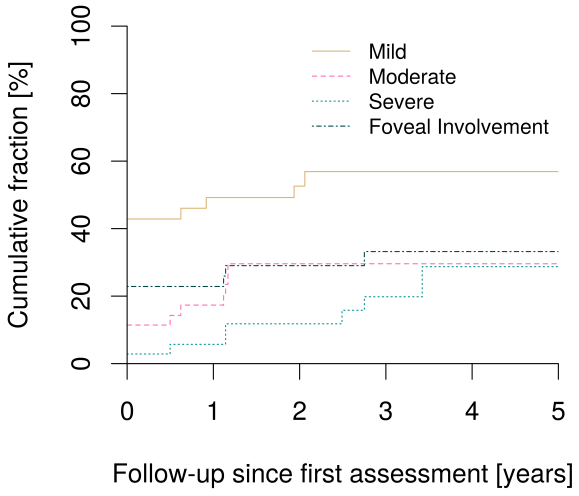

B